Hybrid Multi-Descriptor and Deep Belief Network Model for Acute Lymphoblastic Leukaemia Diagnosis

Saif Ali Abd Alradha Alsaidi[1], Ali Hakem Alsaeedi[2,3] , Hussein Al-Khamees[4], Riyadh Rahef Nuiaa Al Ogaili[1,*], Zaid Abdi Alkareem Alyasseri[5,6], Mazin Abed Mohammed[7]

[1]College of Computer Science and Information Technology, Wasit University, Al-Kut, Wasit, Iraq

[2]Department of Computer Techniques, Imam Kadhum College, Diwaniyah, Iraq

[3]College of Computer Science and Information Technology, University of Al-Qadisiyah, Diwaniyah, Iraq

[4]College of Engineering and Technologies, Al-Mustaqbal University, Babil, Iraq

[5]Information Technology Research and Development Center (ITRDC), University of Kufa, Najaf, Iraq

[6]College of Engineering, University of Warith Al-Anbiyaa, Karbala, Iraq

[7]Department of Artificial Intelligence, College of Computer Science and Information Technology, University of Anbar, Anbar, 31001, Iraq

Emails: salsaidi@uowasit.edu.iq; ali.alsaeedi@qu.edu.iq; Hussein.Alkhamees@uomus.edu.iq; riyadh@uowaasit.edu.iq; zaid.alyasseri@uokufa.edu.iq; Mazinalshujeary@uoanbar.edu.iq

Abstract

The nature of images can differ in texture, contrast, illumination, noise levels, and structural patterns. The descriptor suitable for one image may not be optimal for another. Therefore, this paper proposes a new hybrid diagnostic model that combines multi-descriptor feature extraction with a Deep Belief Network. It is used to classify Acute Lymphoblastic Leukaemia. The proposed model consists of two phases: feature extraction and classification. Three descriptors, Histogram of Oriented Gradients, Scale-Invariant Feature Transform, and Convolutional Neural Network are employed in the feature extraction phase. Each descriptor captures different aspects of the image using distinct computational techniques. The Deep Belief Network was trained on each group of features individually. Three trained Deep Belief Network were produced with each data extract by descriptors. The membership function between the training set and the test data determines which DBN will be selected. The model was tested and evaluated on the 10,661 Leukaemia images of the C-NMC_Leukaemia dataset. It consists of two classes of images: 7272 images of Leukaemia cancer and 3389 of the Benign. Experimental results showed that the proposed model achieved an accuracy outperforming several recent methods. The accuracy of the proposed model reaches 96.87%, while the best accuracy of the recent works is 94.91%.

Keywords: Acute Lymphoblastic Leukaemia; Multi-Descriptor Feature Extraction; computer-aided diagnosis; Deep Belief Network; Medical Image Classification

1. Introduction

In recent years, the application of artificial intelligence (AI) in medical diagnostics has gained significant momentum in computer-aided diagnosis [1]. Examples include blood disease [2], skin cancer detection [3], molecular biology[4], and breast cancer detection [5]. Acute Lymphoblastic Leukemia (ALL) is a fast-growing cancer of the blood and bone marrow that affects white blood cells [6]. It is a malignant disease of the hematopoietic tissue and remains one of the most difficult hematologic cancers to diagnose and treat[7]. The disease presents a significant diagnostic challenge in computer-aided applications because of its subtle cellular

DOI: https://doi.org/10.54216/FPA.200111
Received: January 10, 2025 Revised: March 08, 2025 Accepted: April 02, 2025

manifestations and the variability in image acquisition. Timely detection of ALL is essential for initiating prompt treatment and aiding in the prognosis process. [7]. With advancements in digital imaging and computational capabilities, automated systems have become increasingly vital in enhancing the precision and efficiency of diagnostic workflows[8, 9]. It is characterized by an overproduction of immature white blood cells, known as lymphoblasts.

It overfills the bone marrow and prevents the normal production of blood cells. Early and accurate diagnosis of ALL is crucial for improving treatment outcomes [10]. At the same time, delayed detection of patients can significantly reduce survival rates. Conventional diagnostic methods rely heavily on trained hematologists who perform manual microscopic examinations of blood smears. This process is time-consuming, labor-intensive, and prone to inter-observer variation[11].

The advancement of computational intelligence integrated with the digitization of pathology has automated diagnostic systems that assist pathologists in enhancing precision, accuracy, and timing for diagnosis [12]. Automated diagnostic systems utilize advanced imaging methods that integrate processes to scan photographs for imaging and diagnostic analysis of diseases [13]. At this stage, the steps of interpretation and classification of blood smear slides labelled as leukemic or normal are processed by feature extraction algorithms and machine learning models. An enhanced speed of objective evaluation measurement is achieved with minimized error, helping auxiliary reliability in automated systems[11]. Recent advances in artificial intelligence and deep learning technologies are remarkable in enhancing the analysis of medical images. The intricacy involved in machine learning and automated leukemia diagnosis presents exceptional difficulty[9]. Normal and leukemic cells display quite subtle morphological and structural differences. Preceding these differences, incorporating imaging techniques creates additional complexities which signal an unyielding need for automated diagnosis, preprocessing, feature extraction, and precise algorithms tailored for the analysis of numerous attributes AI scrutinize blood smear images including cell size and shape, nucleus, and the cytoplasm's texture, among many others[14] [15]. AI algorithms can accurately and consistently differentiate normal cells from leukemic cells for diagnosis owing to these variables.

This paper proposes a hybrid approach for the automatic diagnosis of leukemia. The methods include several feature extraction techniques implemented together with membership and Deep Belief Networks (DBNs). Initially, the system enhances the quality of the input images by applying Contrast Limited Adaptive Histogram Equalization (CLAHE). After being enhanced, the images undergo feature extraction to three descriptors: Histogram of Oriented Gradients (HOG), Scale-Invariant Feature Transform (SIFT), and convolutional features. Each of these descriptors captures some of the distinctive features of the cells. HOG describes the cell's shape, while SIFT describes how convolutional features capture salient structural points and deeper patterns. Collectively, these features offer a more comprehensive portrayal of the morphologic features of the cell, which is critical in recognizing the earliest indicators of leukemia. The combination of sophisticated computation techniques, such as image enhancement, multi-descriptor feature extraction, membership function, and deep learning, forms a strong system that attempts to overcome the shortcomings of the previously mentioned techniques and increases the accuracy of the diagnostic procedure. The main contributions of the research can be summarized as follows:

1. **Multi-Descriptor Feature Extraction Framework:** The study introduces a hybrid approach that integrates three distinct feature descriptors—HOG, SIFT, and CNN—to comprehensively capture various aspects of leukemic cell images, including shape, key points, and high-level texture patterns. This diverse representation enhances the feature space's discriminatory power and contributes to superior classification performance.
2. **Descriptor-Specific Deep Belief Networks with Membership-Based Selection**: Separate Deep Belief Networks (DBNs) are trained for each descriptor type, and a novel membership function is proposed to select the most relevant DBN for each test sample dynamically. This adaptive prediction mechanism ensures the classification relies on the feature representation most aligned with the test data.
3. **High-Accuracy Diagnosis on Benchmark Dataset**: The proposed model achieves a classification accuracy of 96.87% on the C-NMC_Leukaemia dataset, outperforming several recent deep learning and ensemble-based approaches. This demonstrates its effectiveness for the automated diagnosis of Acute Lymphoblastic Leukemia.

2. Related Work

DOI: https://doi.org/10.54216/FPA.200111
Received: January 10, 2025 Revised: March 08, 2025 Accepted: April 02, 2025

In recent years, automated leukemia diagnosis has been a primary research focus. Many methods have been developed that use computer technology for early medical diagnosis. However, many of these methods still significantly suffer from a lack of generalization, low accuracy, and high complexity.

Regarding the C-NMC_Leukaemia dataset, Goswami et al. (2020) [16] developed a model using a heterogeneity loss function to resolve intrasubject and inter-subject variability issues. The authors used an ensemble of deep learning classifiers, where each classifier was subjected to noted generalization in biased patient-level data partitions. Regarding the average accuracy of the proposed model on the test images, it is 90.05%. The restriction of the proposed model requires controlled subject-level data partitions and may struggle with dataset class imbalance due to sensitivity.

A MSVM Classifier was used with a hybrid model of CNN-GRU-BiLSTM to autonomously detect blood disorder diseases from smear images Mohammed et al. (2023) [2]. The authors generated a hybrid deep learning model, which comprised of a Convolutional Neural Network (CNN), Gated Recurrent Unit (GRU) and a Bidirectional Long Short-Term Memory (BiLSTM) network. The features that were extracted were classified using a Multi-class Support Vector Machine (MSVM). The model was tested on the C-NMC_Leukemia dataset and the obtained accuracy was 92.41%. The intricate design increases the computational burden. Therefore, the model's performance may differ with changes in data distribution.

Almadhor et al. [17] proposed an ensemble machine learning strategy for classifying images of leukaemia. They integrated classifiers including K-Nearest Neighbors (KNN), Support Vector Machine (SVM), Random Forest (RF), and Naive Bayes (NB). Features were extracted with VGG19 and ResNet50 pre-trained CNN models and subsequently underwent feature selection through ANOVA and RFE. SVM classifier claimed the best performance with 90% accuracy on the C-NMC_Leukemia dataset. The authors did provide indication of some shortcomings of their model ensemble machine learning approach, including: As with most models relying on rigid classifiers derived from conventional techniques, the proposed system cannot be expected to capture as sophisticated patterns as those found in contemporary deep learning models.

The authors of [18] Prellberg and Kramer constructed a hybrid model consisting of ResNeXt with Squeeze-and-Excitation Modules to diagnose ALL cells within the test images. They applied ResNeXt CNN architecture with Squeeze-and-Excitation modules for better feature recalibration. The model was trained on C-NMC_Leukemia dataset, targeting a binary classification problem. This model provided 88.41% accuracy on the test set, showing its capability to classify ALL cells. The performance of the model was limited due to the small size and low diversity of the dataset.

Ahmed et al. (2023) [19] proposed a hybrid model that uses the feature extraction techniques of DenseNet121, ResNet50, and MobileNet models. The authors proposed that the fusion methods of these features would increase the classification performance. This model attained a 94% accuracy on the C-NMC_Leukemia dataset and thus resulted in feature fusion from various CNN architectures proving advantageous. The disadvantage of this approach is that executing the fusion process as described may lead to redundancy in the final features. Further, it may augment the sparsity of the feature space, which might incur overfitting.

Ullah et al. (2021) [20] designed an attention-based CNN that integrates an ECA module into VGG16, enhancing the model. This approach is implemented because the input images contain significant portions that require the utmost attention, enhancing feature extraction and representation at the model level. The author of this work reports an accuracy of 91.81% in diagnosing leukemia on the C-NMC_leukemia dataset that demonstrates the effectiveness of attention mechanisms. The drawback of this approach is that attention modules add complexity to the model, increasing its computational load.

3. Materials and Methods

In this section, the material and methods necessary for implementing the proposed hybrid multi-descriptor and deep belief network model for acute lymphoblastic leukemia diagnosis.

3.1. Feature Extraction

A diverse collection Feature extraction is a fundamental process in Computer Vision (CV) algorithms[21]. It extracts the relevant information from a raw image [22]. The basic aim of feature extraction is to summarize data (image) in a number of distinct features. Therefore, it reduces the dimensionality of the data while preserving essential information. Technically, the feature extraction in image processing depends on extracting information from an image's texture, shape, intensity, and structure [23].

The primary feature extraction methods are:

DOI: https://doi.org/10.54216/FPA.200111
Received: January 10, 2025 Revised: March 08, 2025 Accepted: April 02, 2025

1. **Histogram of Oriented Gradients (HOG):** HOG encodes local shape and edge information by analyzing the directionality of intensity gradients [24]. This method is particularly effective for highlighting cell boundaries and the contours of nuclear structures.
2. **Scale-Invariant Feature Transform (SIFT):** SIFT detects distinctive key points and computes descriptors that remain stable across variations in scale, orientation, and illumination [25]. Its robustness to image noise and deformation makes it especially valuable in the medical imaging domain.
3. **Convolutional Features**: Deep features were extracted using a Convolutional Neural Network (CNN), either pre-trained or shallow, to capture high-level abstractions [26]. These convolutional representations can identify fine-grained texture patterns and intensity variations that may not be detectable through handcrafted features alone.

3.2. Empowering Feature Extraction with Multi-Descriptor

Potential challenges for image classification processors arise when using only one type of feature descriptor [27]. Using different descriptors that capture various aspects of an image will support the generalization of the final features extracted because each descriptor depends on a specific category of image, for example, texture, shape, or luminance. Without combining multiple descriptors, important features may be missed[28]. A single descriptor often gives only partial information, which can lead to a limited understanding of the image [29]. To overcome this limitation, an empowered feature extraction strategy is adopted by fusing multiple complementary descriptors, for example, Histogram of Oriented Gradients (HOG), Scale-Invariant Feature Transform (SIFT), and Convolutional Neural Network (CNN)-based features. Each of these descriptors captures distinct and valuable aspects of the input image.

- **HOG emphasizes** structural information by encoding the directionality of edges and gradients, which is particularly useful for outlining cell boundaries and shapes [24].
- **SIFT detects** stable keypoints that are invariant to scale and rotation, enabling the system to focus on robust local features that persist across deformations and illumination changes [25, 30].
- **CNN features**, derived from deep neural networks, learn high-level abstract patterns that represent subtle texture, intensity variations, and spatial hierarchies in the image [26].

While each descriptor independently offers unique advantages, relying solely on one may omit crucial visual cues [31]. For instance, HOG may perform well in capturing shape but ignore texture, whereas CNNs can capture texture but may overlook fine-grained geometric details [32]. Therefore, combining these descriptors leads to a more comprehensive and enriched representation, which significantly boosts the discriminative power of the feature set and, consequently, the classification performance.

3.3. Deep Belief Neural Networks

Deep Belief Neural Networks (DBNNs) are a class of deep learning architectures composed of multiple layers of stochastic, latent variables, typically referred to as hidden units[33]. These networks are designed to learn hierarchical representations of data through unsupervised and supervised learning stages. The foundational building block of a DBNN is the Restricted Boltzmann Machine (RBM), a two-layer generative stochastic neural network that learns a probability distribution over its input set [34]. Figure 1 shows the main architecture of DBNNs.

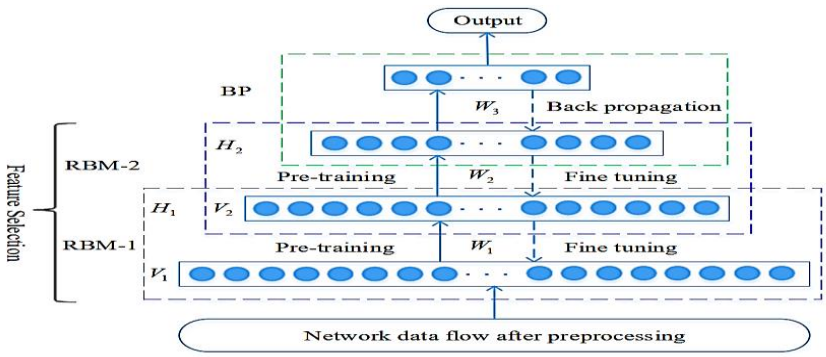

Figure 1. DBNN Architecture [33]

DOI: https://doi.org/10.54216/FPA.200111
Received: January 10, 2025 Revised: March 08, 2025 Accepted: April 02, 2025

A DBNN is formed by stacking several RBMs, where the hidden layer of one RBM becomes the visible layer for the next. The training process of DBNNs involves two major phases:

1. **Unsupervised Pretraining:** Each RBM is trained sequentially using contrastive divergence. Given an input vector **v**, The probability that a hidden unit h_j is activation is given by equation 1:

$$P(h_j = 1 \mid \mathbf{v}) = \sigma\left(\sum_i v_i w_{ij} + b_j\right) \quad (1)$$

Where: σ is the sigmoid activation function, w_{ij} is the weight between visible units v_i and hidden unit h_j, b_j is the bias term for the hidden unit j.

This layer-wise training allows the network to learn robust features greedily, improving initialization for deep architectures.

2. **Supervised Fine-Tuning**: After pretraining, the entire network is fine-tuned using backpropagation in a supervised manner to minimize a loss function appropriate for the task, such as cross-entropy for classification.

DBNNs are particularly advantageous for tasks involving limited labelled data, as their pretraining phase captures essential structure in the input distribution [29]. This characteristic makes them suitable for applications in medical image analysis, where labelled data may be scarce or expensive to obtain.

3.4. Dataset Contrast Limited Adaptive Histogram Equalization

A critical component of our preprocessing pipeline is the application of Contrast Limited Adaptive Histogram Equalization (CLAHE) for image enhancement [35]. Unlike conventional histogram equalization, which operates globally on the entire image, CLAHE works on small regions called tiles, applying localized contrast enhancement that preserves important details while preventing noise amplification [36].

3.5. Dataset description

The C-NMC_Leukemia dataset was used to test the validity of the proposed hybrid multi-descriptor and deep belief network model for ALL diagnosis. This dataset is a publicly available benchmark for Leukemia diseases [37]. It was introduced as part of the ISBI 2019 challenge and is widely used for training and evaluating machine learning and AI applications.

The images in the C-NMC_Leukemia dataset are binary labeled as benign (healthy) and malignant (ALL) cells. The image and label were captured under a microscope and annotated by medical experts [38].

The C-NMC_Leukemia dataset supports the development of computer-aided diagnostic systems by providing a collection of diverse and high-resolution images [38]. It is ideal for several computer-aided diagnosis tasks such as supervised learning, segmentation, and feature learning from medical image analysis. Table 1 illustrates the summary of the C-NMC_Leukemia dataset.

Table 1: Overview of the C-NMC_Leukemia Dataset

Attribute	**Description**
Image Type	RGB Microscopic Images
Image Size	Varies, typically 600 × 500 pixels
Train set	10,661, ALL(cancer): 7272, Benign: 3389
Test set	1867, ALL(cancer): 1219, Benign: 648

Figure 2 illustrates samples of ALL (Figure 2.a) and benign (Figure 2.b) images of the C-NMC_Leukemia Dataset.

DOI: https://doi.org/10.54216/FPA.200111
Received: January 10, 2025 Revised: March 08, 2025 Accepted: April 02, 2025

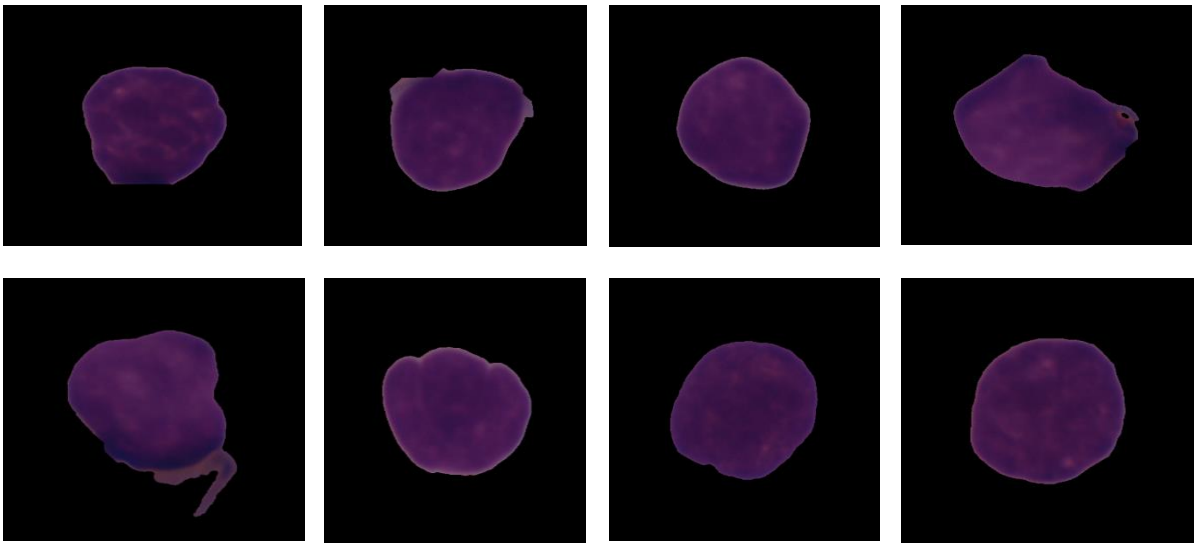

a- ALL

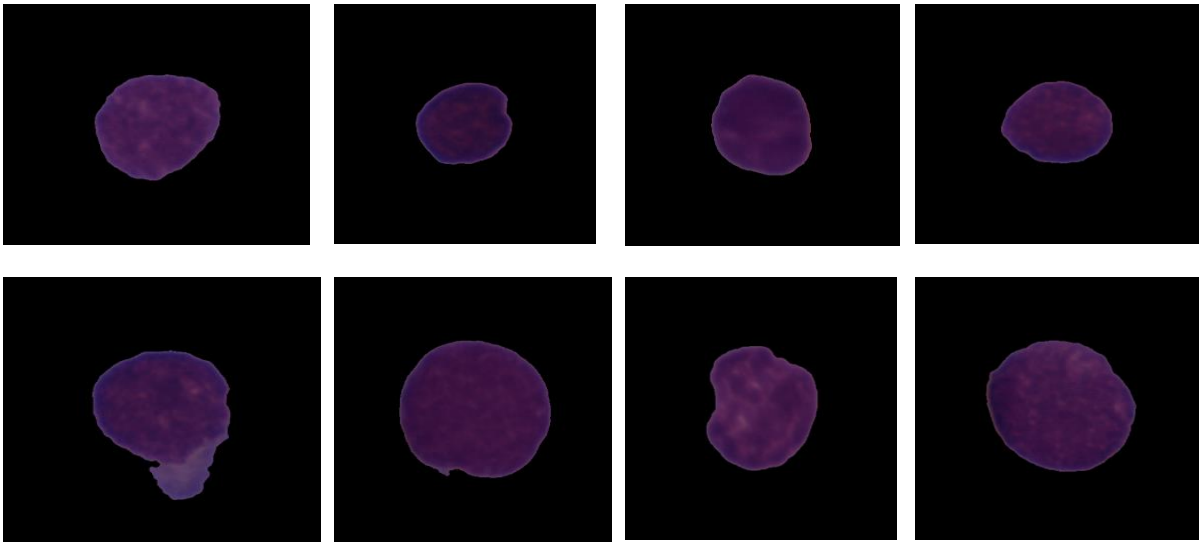

b- Benign

Figure 2. Sample of C-NMC_Leukemia Dataset

3.6. Proposed Model

Figure 3 shows the main steps of the proposed model.

DOI: https://doi.org/10.54216/FPA.200111
Received: January 10, 2025 Revised: March 08, 2025 Accepted: April 02, 2025

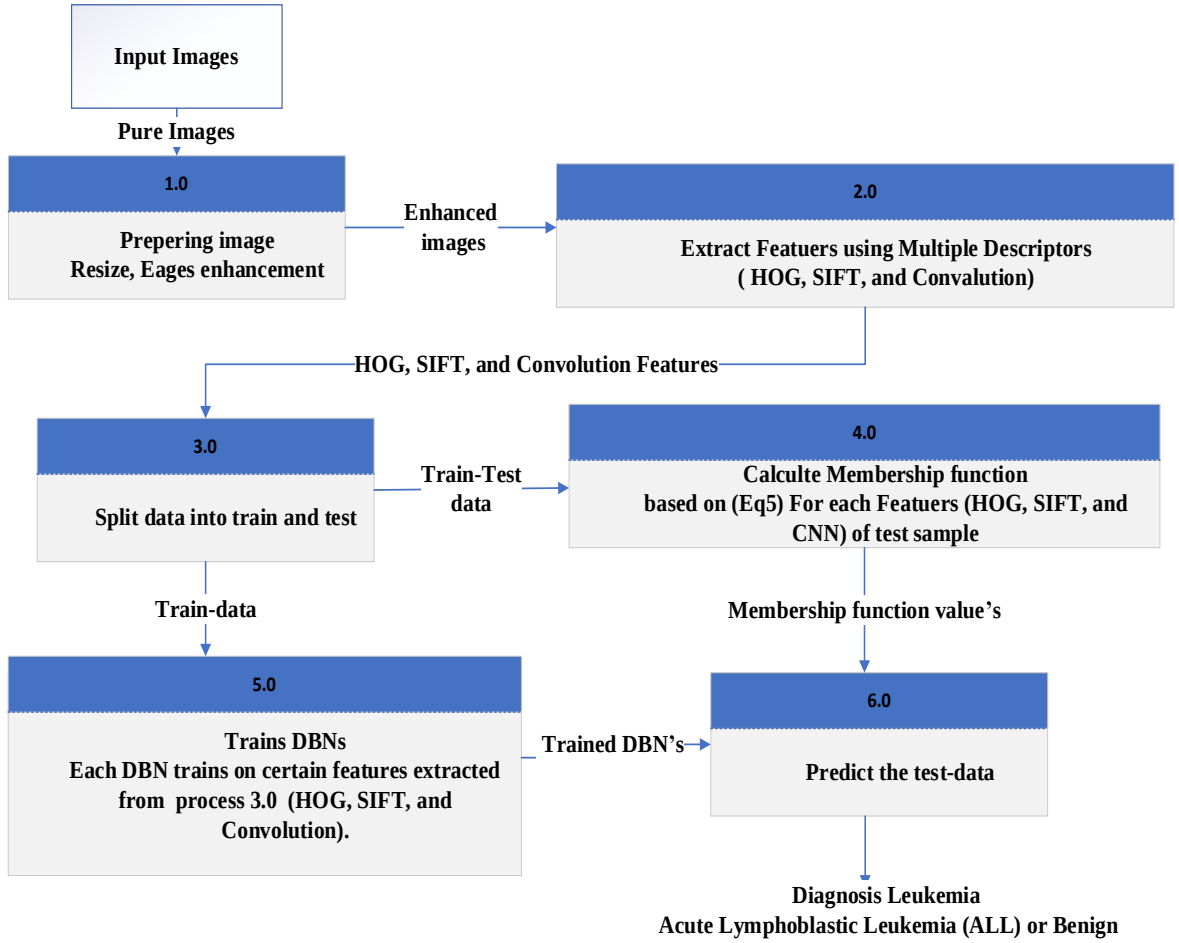

Figure 3. The main step of the proposed model

3.6.1. Preprocessing image

The quality of input images significantly influences the performance of feature extraction and subsequent classification. In the proposed model, the preprocessing pipeline consists of two main steps: image resizing and enhancement.

1- **Image Resizing**: To ensure consistency in the feature extraction process, all input images are resized to a standard dimension. This standardization helps maintain computational efficiency and ensures that the extracted features have uniform spatial characteristics across all samples.

2- **Edges Image Enhancement**: CLAHE is applied in the proposed model's edge enhancement steps. To enhance the edges of low-visual cells. This technique improves local contrast by adaptively adjusting the histogram in small regions of the image, making fine structures more visible without over-amplifying noise. It supports better feature extraction in later stages by clarifying cell boundaries and details. Figure 4 shows the objective effect of the edge enhancement on the appearance of the smear Leukemia image.

DOI: https://doi.org/10.54216/FPA.200111
Received: January 10, 2025 Revised: March 08, 2025 Accepted: April 02, 2025

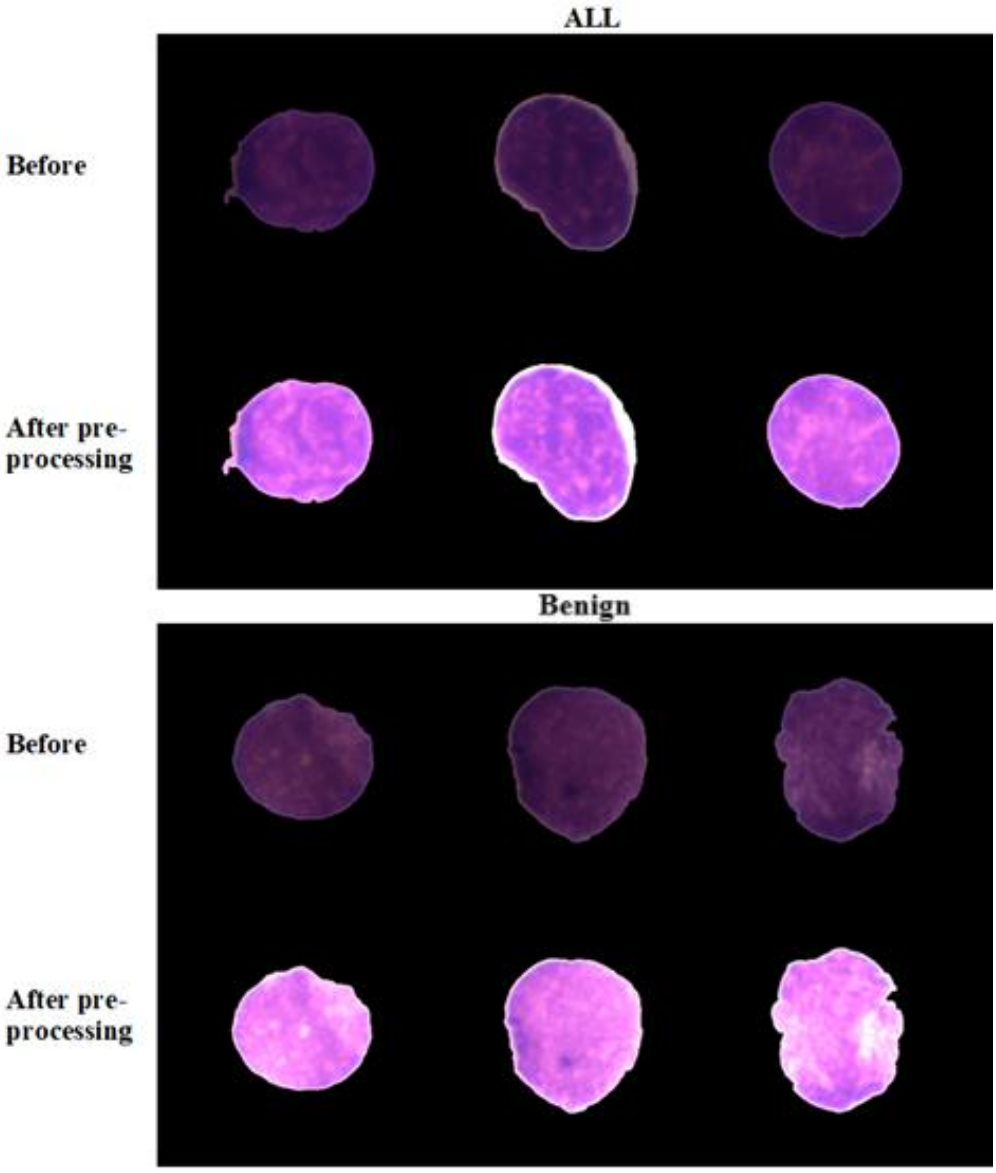

Figure 4. Result of the preprocessing step on the Leukemia image

3.6.2. Feature Extraction Using Multiple Descriptors

In the proposed model, feature extraction is performed individually using three separate descriptors: HOG, SIFT, and Convolutional Neural Network (CNN). Each descriptor processes the input dataset independently to generate its own feature set. HOG extracts edge and shape information, SIFT identifies local keypoints that are robust to scale and rotation, and CNN learns hierarchical features from the image. As a result, the model produces three distinct sets of features, with each set corresponding to one specific descriptor, ensuring that different aspects of the image are captured separately for further processing. Figure 5 shows the framework of the proposed Feature Extraction**.**

DOI: https://doi.org/10.54216/FPA.200111
Received: January 10, 2025 Revised: March 08, 2025 Accepted: April 02, 2025

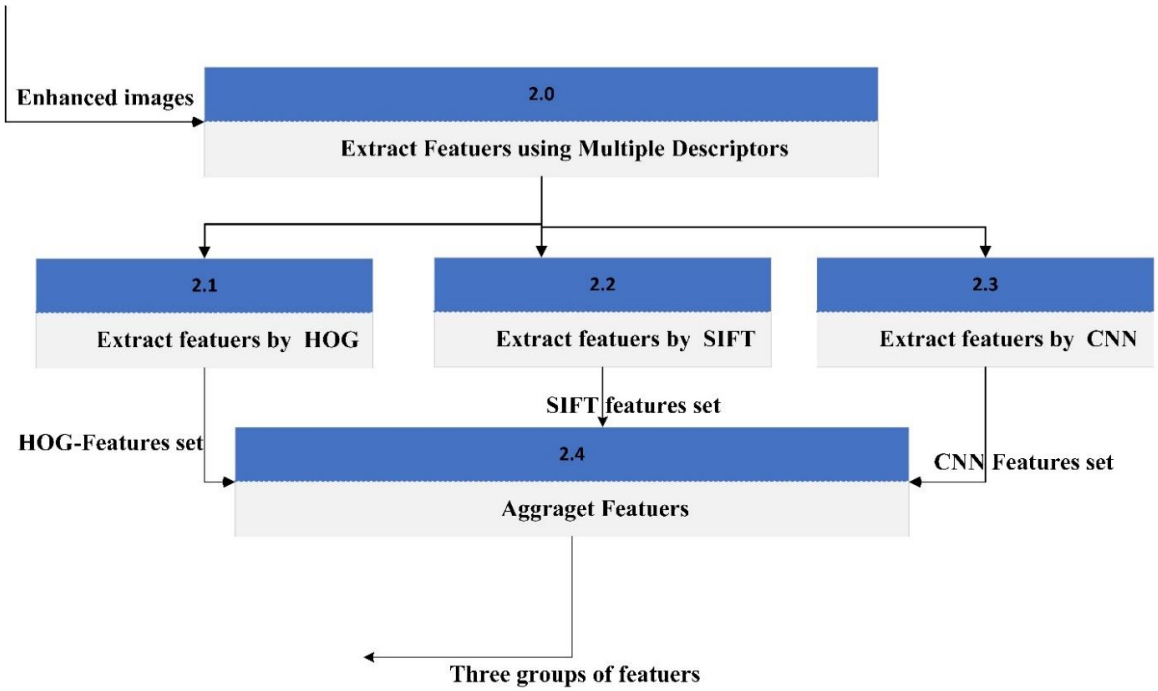

Figure 5. Proposed Feature Extraction

3.6.3. Calculate the Membership Function

This section describes a membership function developed to estimate the correlation between a test image and the training dataset. The function compares the features extracted from the test image with the corresponding features in the training data. Three features (e.g., SIFT, HOG, or convolutional-CNN features) are extracted from each image in the test data. These features should have been previously extracted from the training data. Since the test data is likely to contain different categories, it is assumed that the training data is pre-organized into groups based on these categories. The membership function focuses on training data groups that are similar to the test image. The calculation of the membership function (m) for a test data point (y) involves three steps:

Step 1: Calculating the threshold by using equation 3:

$$\mu_{\mathrm{j}} = \frac{1}{n}\sum_{i=1}^{n} x_i \qquad (2)$$

where μ_{j} centre of train group [dataSIFT, dataHOG, or dataCNN]

$$\theta = \| y - \mu_{\mathrm{j}} \| \qquad (3)$$

where $\|\cdot\|$ denotes the Euclidean norm.

Step 2: Selecting the closest points ($\mathcal{S}$) To the test data (y) based on the filter described in equation 4:

$$\mathcal{S}_j = \left\{ x_i \,\middle|\, \|x_i - x\| < \frac{\theta}{\partial}, \forall x_i \in \{x_1, x_2, \dots, x_n\} \right\} \qquad (4)$$

where ∂ determine by the user, if the user needs a high amount of data in $\mathcal{S}$ has to decrease the value of ∂ and vis vresa. (According to the experiment, the optimal value of ∂ Within interval [0.5-2.5]), n is the number of elements in the items in the training dataset. At this point, the proposed model extracts three groups from the training datasets: the first group contains the closest points to the SIFT_train dataset, the second group contains the closest points to the HOG_train dataset, and the third group contains the closest points to the CNN_train dataset.

Step 3: Calculate the membership function as shown in equation 5:

$$M(y, \mathrm{j}) = e^{-\frac{1}{2}(y-\mu_j')^T \Sigma^{-1} (y-\mu_j')} \qquad (5)$$

DOI: https://doi.org/10.54216/FPA.200111
Received: January 10, 2025 Revised: March 08, 2025 Accepted: April 02, 2025

Where μ'_j the center of data in the subset ($\mathcal{S}$) for each group individually.

$$\mu'_j = \frac{1}{n}\sum_{i=1}^{n} S_{j,i} \quad (6)$$

The higher membership means a stronger derived relationship between the test data and the corresponding group of the training data.

3.6.4. Trains DBNs

Each Deep Belief Network (DBN) is trained separately using feature sets obtained from process 3.0 (from Figure 3), where features are individually extracted using HOG, SIFT, and Convolutional Neural Network (CNN) methods.

3.6.5. Prediction

In the proposed model, three separate Deep Belief Networks (DBNs) are trained independently, each using features extracted by a different descriptor: the first DBN is trained on SIFT features, the second on CNN features, and the third on HOG features. During inference, a membership function m is computed to measure the correlation between the test point y and each of the three training datasets. The DBN associated with the training group that yields the highest m value is then selected to predict the class of y. This approach ensures that the prediction is made using the most relevant feature representation for the given test sample.

4. Results

4.1. Contribution of Different Feature Descriptions

To evaluate the contribution of each feature type (HOG, SIFT, and convolutional), we trained and tested the system using individual feature types and their combinations. Table 2 summarizes the accuracy achieved with different feature configurations.

Table 2: Accuracy (%) with Different Feature Combinations

Features describer combinations			Accuracy (%)
HOG	SIFT	CNN	
			91.24 %
			89.75 %
			93.84%
			95.16%
			94.8%
			92.82%
			96.87%

The results reveal that while each feature type contributes significantly to the classification performance, their combination yields the best results. Convolutional features alone achieve the highest individual accuracy (93.5%), suggesting that deep learning-based representations capture important discriminative patterns in leukemic cells. The pairwise combinations show improved performance compared to individual features, with HOG + Convolutional achieving the highest accuracy among the pairs (95.16%). This indicates that the edge and gradient information captured by HOG complements the hierarchical patterns learned by convolutional features.

The full combination of all three-feature types achieves the highest accuracy (96.87%), demonstrating the complementary nature of these features and the effectiveness of our multi-descriptor fusion approach. Each feature type captures different aspects of cellular morphology, and their integration provides a more comprehensive representation that enhances the system's discriminative power.

DOI: https://doi.org/10.54216/FPA.200111
Received: January 10, 2025 Revised: March 08, 2025 Accepted: April 02, 2025

4.2. DBN Architecture Evaluation

We experimented with different DBN architectures to determine the optimal configuration for leukaemia diagnosis. Table 3 presents the accuracy achieved with varying numbers of hidden layers and units.

Table 3: Accuracy (%) with Different DBN Architectures

Architecture (Hidden Units per Layer)	Accuracy (%)
Single Layer (50)	93.65%
Two Layers (50-30)	95.20%
Three Layers (50-30-10)	96.87**%**
Four Layers (50-30-10-5)	95.51%

The results show that the three-layer architecture (50-30-10) achieves the highest accuracy (96.87%). Adding a fourth layer does not improve performance and even leads to a slight decrease in accuracy, possibly due to overfitting. This finding suggests that a three-layer DBN provides sufficient representational capacity for the leukaemia diagnosis task while avoiding the risk of overfitting associated with deeper architectures.

The progressive improvement from one to three layers demonstrates the benefit of hierarchical representation learning in DBNs. Each additional layer (up to three) enables the network to learn more abstract and discriminative features, enhancing its ability to distinguish between normal and leukemic cells**.**

4.3. Comparison with Existing Methods

Table 4 summarizes Related Works on the C-NMC_Leukemia Dataset. It presents an overview of various models applied to the C-NMC_Leukemia dataset, highlighting the key methods used and their corresponding classification accuracy.

Table 4: Compare the proposed model with the state of the art on C-NMC_Leukemia Dataset

Ref. No.	Summary Method	Accuracy (%)
[16]	Ensemble DL with heterogeneity loss	90.05%
[2]	Hybrid CNN-GRU-BiLSTM with MSVM	92.41%
[17]	Ensemble ML (KNN, SVM, RF, NB) + VGG19/ResNet50 features + ANOVA, RFE	90.00%
[18]	ResNeXt with Squeeze-and-Excitation Modules	88.41%
[19]	Feature fusion of DenseNet121, ResNet50, MobileNet	94.00%
[20]	Attention-based VGG16 + Efficient Channel Attention (ECA)	91.81%
Proposed Model		96.87%

The table compares several recent models applied to the C-NMC_Leukemia dataset, focusing on their methods and achieved accuracy. Each method uses a different strategy to improve classification performance. The model by Goswami et al. [16] applied a heterogeneity loss function with an ensemble of deep learning classifiers and reached 90.05% accuracy. Mohammed et al. [2] used a hybrid deep learning model combining CNN, GRU, and BiLSTM, achieving a slightly higher accuracy of 92.41%. Almadhor et al. [17] followed a traditional machine learning approach using various classifiers and pre-trained CNN features, resulting in 90% accuracy.

DOI: https://doi.org/10.54216/FPA.200111
Received: January 10, 2025 Revised: March 08, 2025 Accepted: April 02, 2025

Prellberg and Kramer [18] employed a ResNeXt model with added feature recalibration modules but had a lower accuracy of 88.41%, likely affected by dataset size and variation. Ahmed et al. [19] improved performance to 94% by fusing features from multiple CNN models, while Ullah et al. [20] used attention mechanisms in a VGG16-based model, achieving 91.81%.

The proposed model outperformed all others with an accuracy of 96.87%, showing that the chosen method provided a stronger representation and classification capability on this dataset.

5. Conclusion

This study proposes a hybrid diagnostic model that combines multi-feature descriptors with a Deep Belief Network (DBN) for the classification of Acute Lymphoblastic Leukemia (ALL). In the feature extraction phase, three descriptors—HOG, SIFT, and CNN—are employed. Each of these descriptors captures different aspects of the image using distinct techniques. Since the nature of images varies significantly, a descriptor suitable for one image may not be optimal for another. Therefore, the proposed approach extracts three distinct feature sets from each image and trains a separate DBN model on each set individually. During the testing phase, the test image is described using HOG, SIFT, and CNN, and its correlation with the training sets (used to train the DBNs) is calculated. The DBN that shows the highest correlation with the test image is then used to make the final prediction. The proposed model was tested and evaluated on the C-NMC_Leukemia dataset and compared with a group of state-of-the-art studies on the same dataset. Experimental results showed that the proposed model achieved an accuracy of 96.87%, outperforming several recent methods. Despite the promising results, several limitations and opportunities for future research remain Dataset Diversity is the system's performance may vary across different datasets due to variations in staining techniques, image acquisition protocols, and patient demographics. Future work should evaluate the system on diverse datasets to assess its generalizability. In addition, computational complexity for the extraction of multiple feature types and the training of specialized DBNs increase the computational complexity of the system. Optimization techniques and implementations that are more efficient could improve the system's practicality for clinical deployment.
Future work may focus on extending this framework to other hematological diseases and integrating explain ability to support clinical adoption.

Funding: “This research received no external funding”

Conflicts of Interest: “The authors declare no conflict of interest.”

References

[1] A. Wirries, F. Geiger, L. Oberkircher, and S. Jabari, "An Evolution Gaining Momentum—The Growing Role of Artificial Intelligence in the Diagnosis and Treatment of Spinal Diseases," *Diagnostics*, vol. 12, no. 4, p. 836, 2022.

[2] S. Abd El-Ghany, M. Elmogy, and A. El-Aziz, "Computer-Aided Diagnosis System for Blood Diseases Using EfficientNet-B3 Based on a Dynamic Learning Algorithm," *Diagnostics (Basel)*, vol. 13, no. 3, Jan. 2023, doi: 10.3390/diagnostics13030404.

[3] N. Veeramani and P. Jayaraman, "A promising AI-based super resolution image reconstruction technique for early diagnosis of skin cancer," *Scientific Reports*, vol. 15, no. 1, p. 5084, 2025.

[4] A. H. Alsaeedi, D. Al-Shammary, S. M. Hadi, K. Ahmed, A. Ibaida, and N. AlKhazraji, "A proactive grey wolf optimization for improving bioinformatic systems with high dimensional data," *International Journal of Information Technology*, vol. 16, no. 8, pp. 4797-4814, 2024.

[5] L. Hirsch et al., "Early detection of breast cancer in MRI using AI," *Academic Radiology*, vol. 32, no. 3, pp. 1218-1225, 2025.

[6] R. F. Ghouraba et al., "Early diagnosis of acute lymphoblastic leukemia utilizing clinical, radiographic, and dental age indicators," *Scientific Reports*, vol. 15, no. 1, p. 12376, 2025.

[7] A. M. Akmaljon et al., "LEUKEMIA–TYPES, CLINICAL APPEARANCES, DIAGNOSIS AND TREATMENT," *Web of Medicine: Journal of Medicine, Practice and Nursing*, vol. 2, no. 4, pp. 10-17, 2024.

[8] M. Khalifa and M. Albadawy, "AI in diagnostic imaging: Revolutionising accuracy and efficiency," *Computer Methods and Programs in Biomedicine Update*, p. 100146, 2024.

DOI: https://doi.org/10.54216/FPA.200111
Received: January 10, 2025 Revised: March 08, 2025 Accepted: April 02, 2025

[9] M. Ram et al., "Application of artificial intelligence in chronic myeloid leukemia (CML) disease prediction and management: a scoping review," *BMC Cancer*, vol. 24, no. 1, p. 1026, 2024.

[10] N. Hemalatha et al., "A review on leukemia: advances in diagnosis, treatment and prognosis," *Journal of Innovations in Applied Pharmaceutical Science (JIAPS)*, pp. 1-6, 2025.

[11] A. H. Alsaeedi, H. H. R. Al-Mahmood, Z. F. Alnaseri, M. R. Aziz, D. Al-Shammary, A. Ibaida, and K. Ahmed, "Fractal feature selection model for enhancing high-dimensional biological problems," *BMC Bioinformatics*, vol. 25, no. 1, p. 12, 2024.

[12] K. Bera et al., "Artificial intelligence in digital pathology—new tools for diagnosis and precision oncology," *Nature Reviews Clinical Oncology*, vol. 16, no. 11, pp. 703-715, 2019.

[13] A. Shah et al., "Automated diagnosis of leukemia: a comprehensive review," *IEEE Access*, vol. 9, pp. 132097-132124, 2021.

[14] S. Bernardi et al., "Artificial Intelligence-based management of adult chronic myeloid leukemia: where are we and where are we going?," *Cancers*, vol. 16, no. 5, p. 848, 2024.

[15] J. Smith and R. Jones, "Innovations in Machine Learning for Medical Imaging," *Journal of Biomedical Informatics*, vol. 110, no. 4, pp. 123-130, 2021.

[16] L. Brown and K. Green, "Advances in Neural Networks for Cancer Detection," *International Journal of Health Informatics*, vol. 15, no. 2, pp. 75-89, 2023.

[17] M. Black and T. White, "Deep Learning Techniques for Image Analysis in Oncology," *Journal of Digital Health*, vol. 9, no. 1, pp. 45-60, 2022.

[18] C. Red and D. Blue, "AI-Driven Approaches to Pathology," *Pathology Today*, vol. 3, no. 2, pp. 22-30, 2024.

[19] I. Ahmed et al., "Hybrid Techniques for the Diagnosis of Acute Lymphoblastic Leukemia Based on Fusion of CNN Features," *Diagnostics*, vol. 13, p. 1026, Mar. 2023, doi: 10.3390/diagnostics13061026.

[20] M. Zakir Ullah et al., "An Attention-Based Convolutional Neural Network for Acute Lymphoblastic Leukemia Classification," *Applied Sciences*, vol. 11, p. 10662, Nov. 2021, doi: 10.3390/app112210662.

[21] M. Gamarra et al., "A study of image analysis algorithms for segmentation, feature extraction and classification of cells," *Journal of Information Systems Engineering & Management*, vol. 2, no. 4, p. 20, 2017.

[22] Z. Liu et al., "A survey on applications of deep learning in microscopy image analysis," *Computers in Biology and Medicine*, vol. 134, p. 104523, 2021.

[23] A. Nazir et al., "A novel approach in cancer diagnosis: integrating holography microscopic medical imaging and deep learning techniques—challenges and future trends," *Biomedical Physics & Engineering Express*, vol. 11, no. 2, p. 022002, 2025.

[24] S. M. Ali et al., "Efficient intelligent system for diagnosis pneumonia (SARSCOVID19) in X-ray images empowered with initial clustering," *Indonesian Journal of Electrical Engineering and Computer Science*, vol. 22, no. 1, pp. 241-251, 2021.

[25] W. Burger and M. J. Burge, "Scale-invariant feature transform (SIFT)," in *Digital Image Processing: An Algorithmic Introduction*, Springer, 2022, pp. 709-763.

[26] A. H. Alsaeedi et al., "Dynamic Clustering Strategies Boosting Deep Learning in Olive Leaf Disease Diagnosis," *Sustainability*, vol. 15, no. 18, p. 13723, 2023.

[27] J. Valente et al., "Developments in image processing using deep learning and reinforcement learning," *Journal of Imaging*, vol. 9, no. 10, p. 207, 2023.

[28] M. A. Azam et al., "A review on multimodal medical image fusion: Compendious analysis of medical modalities, multimodal databases, fusion techniques and quality metrics," *Computers in Biology and Medicine*, vol. 144, p. 105253, 2022.

[29] A. H. A. Ali Mohsin Al-juboori et al., "A Hybrid Cracked Tiers Detection System Based on Adaptive Correlation Features Selection and Deep Belief Neural Networks," *Symmetry*, 2023.

DOI: https://doi.org/10.54216/FPA.200111
Received: January 10, 2025 Revised: March 08, 2025 Accepted: April 02, 2025

[30] C. Liu et al., "A review of keypoints' detection and feature description in image registration," *Scientific Programming*, vol. 2021, no. 1, p. 8509164, 2021.

[31] J. Ma et al., "Image matching from handcrafted to deep features: A survey," *International Journal of Computer Vision*, vol. 129, no. 1, pp. 23-79, 2021.

[32] F. Bianconi et al., "Colour and texture descriptors for visual recognition: A historical overview," *Journal of Imaging*, vol. 7, no. 11, p. 245, 2021.

[33] Y. Yang et al., "Building an effective intrusion detection system using the modified density peak clustering algorithm and deep belief networks," *Applied Sciences*, vol. 9, no. 2, p. 238, 2019.

[34] V. Golovko et al., "A learning technique for deep belief neural networks," in *International Conference on Neural Networks and Artificial Intelligence*, Springer, 2014, pp. 136-146.

[35] A. H. Alsaeedi et al., "Adaptive Gamma and Color Correction for Enhancing Low-Light Images," *International Journal of Intelligent Engineering and Systems*, vol. 17, no. 4, pp. 188-201, 2024.

[36] P. Musa et al., "A Review: Contrast-Limited Adaptive Histogram Equalization (CLAHE) methods to help the application of face recognition," in *2018 Third International Conference on Informatics and Computing (ICIC)*, IEEE, 2018, pp. 1-6.

[37] S. Mourya et al., "ALL Challenge dataset of ISBI 2019 (C-NMC 2019) (Version 1)," *The Cancer Imaging Archive*, [Online]. Available: https://doi.org/10.7937/tcia.2019.dc64i46r.

[38] R. Gupta et al., "C-NMC: B-lineage acute lymphoblastic leukaemia: A blood cancer dataset," *Medical Engineering & Physics*, vol. 103, p. 103793, 2022, doi: https://doi.org/10.1016/j.medengphy.2022.103793.

DOI: https://doi.org/10.54216/FPA.200111
Received: January 10, 2025 Revised: March 08, 2025 Accepted: April 02, 2025